Electronic Supplementary Information for:

Architecting ordered mesoporous materials via additive manufacturing

Anthony Griffin,[a] Isaac Bauer,[a] Paul Smith,[a] Yizhi Xiang,[b] Zhe Qiang[a,*]

[a]School of Polymer Science and Engineering, University of Southern Mississippi, Hattiesburg, MS, 39406, USA

[b]Department of Chemical and Biomedical Engineering, University of Missouri, Columbia, MO, 65211, USA

Corresponding authors: Z. Q. (zhe.qiang@usm.edu)

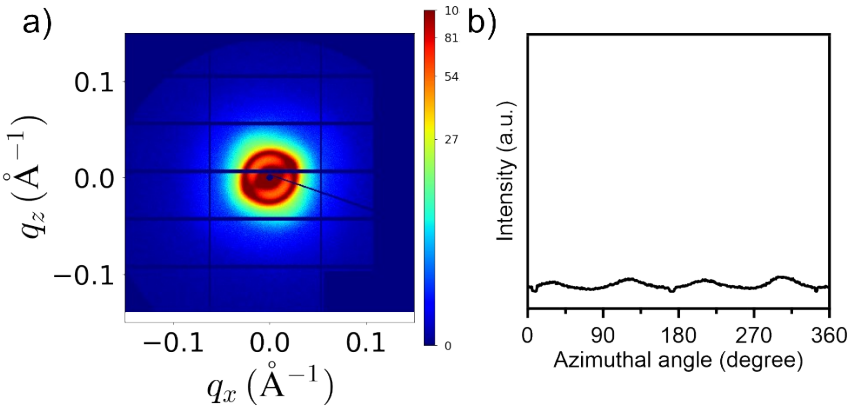

Figure S1. a) 2D SAXS pattern and b) azimuthal angle plot of SEBS:PP (65:35 wt%) after 3D printing

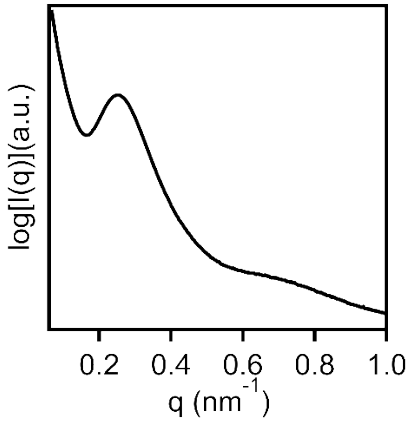

Figure S2. SAXS profile of neat SEBS powder.

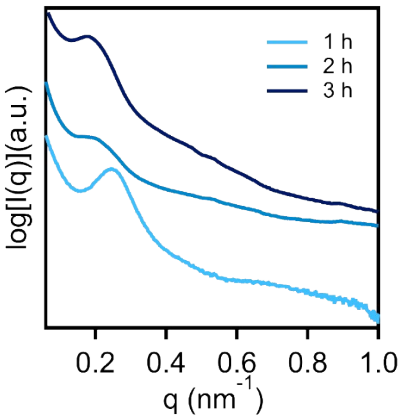

Figure S3. SAXS profiles of 3D polymer prepared from a 65:35 wt% SEBS:PP blend reacted for 1 h, 2 h, and 3 h in sulfuric acid with presence of DCP.

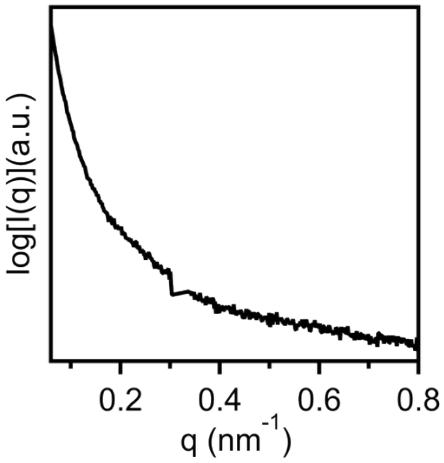

Figure S4. SAXS profile of 3D-structured polymer prepared from a 65:35 wt% SEBS:PP blend reacted for 4 h in sulfuric acid with presence of DCP.

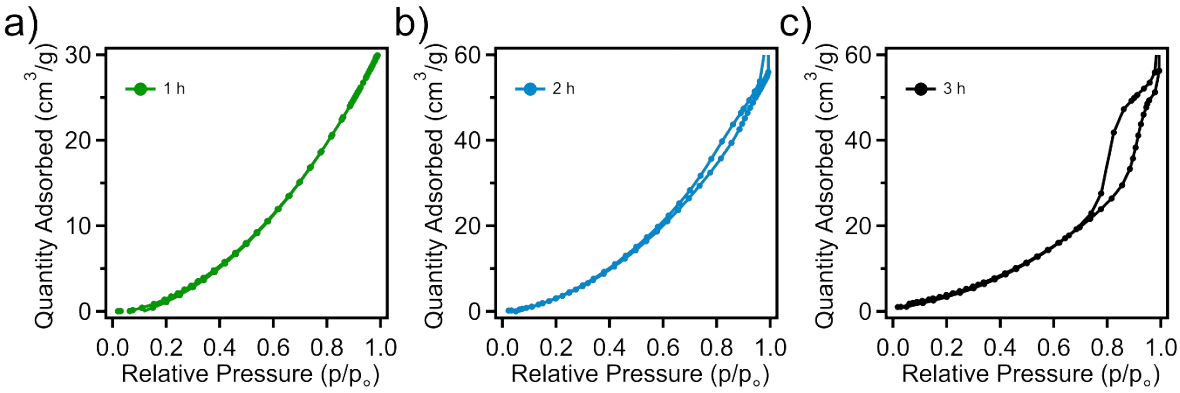

Figure S5. Nitrogen physisorption isotherms of 3D-structured polymer prepared from a 65:35 wt% SEBS:PP blend reacted for a) 1 h, b) 2 h, and c) 3 h in sulfuric acid with presence of DCP.

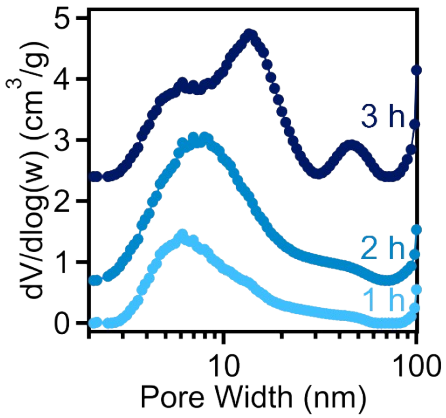

Figure S6. Pore size distributions of 3D-structured polymer prepared from a 65:35 wt% SEBS:PP blend reacted for 1 h, 2 h, and 3 h in sulfuric acid with presence of DCP. Pore size distributions were shifted in the positive Y-direction: 1 h (+0), 2 h (+0.7), and 3 h (+2.4).

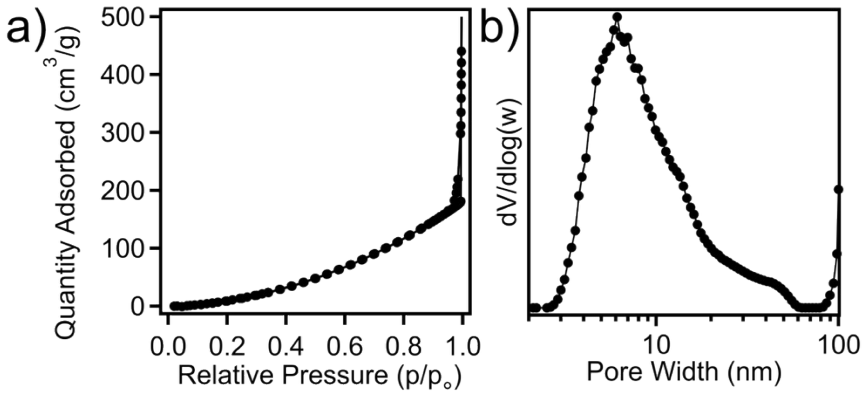

Figure S7. a) Nitrogen physisorption isotherm and b) pore size distribution of 3D polymer prepared from a 65:35 wt% SEBS:PP blend reacted for 4 h in sulfuric acid with presence of DCP.

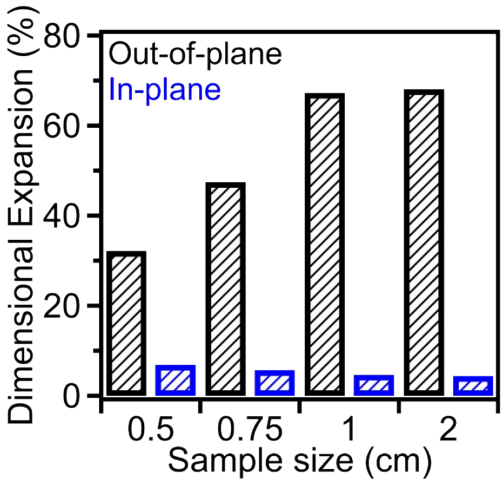

Figure S8. Dimensional change of 3D OMP 3D as a function of printed size; all samples were reacted for 3h in sulfuric acid with the presence of 1wt% DCP.

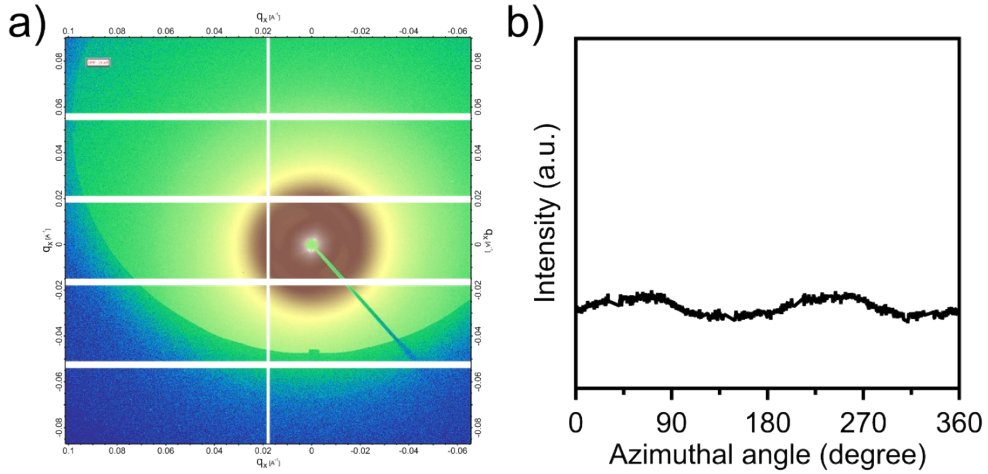

Figure S9. a) 2D SAXS pattern and b) azimuthal angle plot of a 3D-structured OMP prepared from a 65:35 wt% SEBS:PP blend reacted for 3 h.

Figure S10. Images of complex 3D OMP structures.

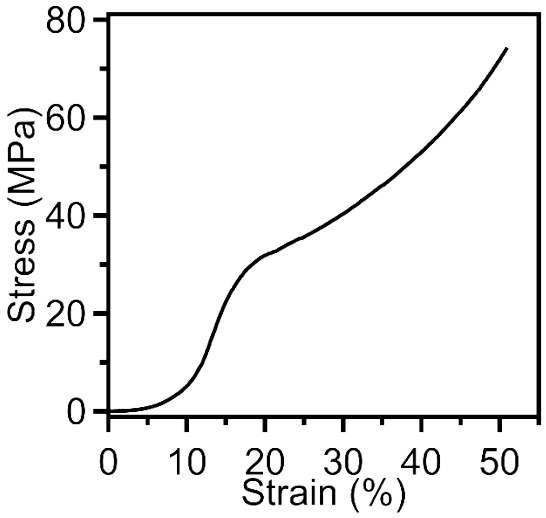

Figure S11. Representative compressive stress-strain curve of a 3D-structured OMP prepared from a 65:35 wt% SEBS:PP blend reacted for 3 h.

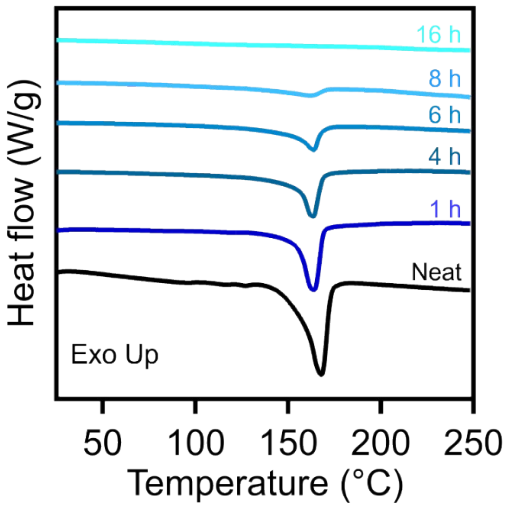

Figure S12. DSC thermograms of the second heating trace for SEBS:PP (65:35 wt%) 3D-structures sulfonated at 135 °C as a function of reaction time.

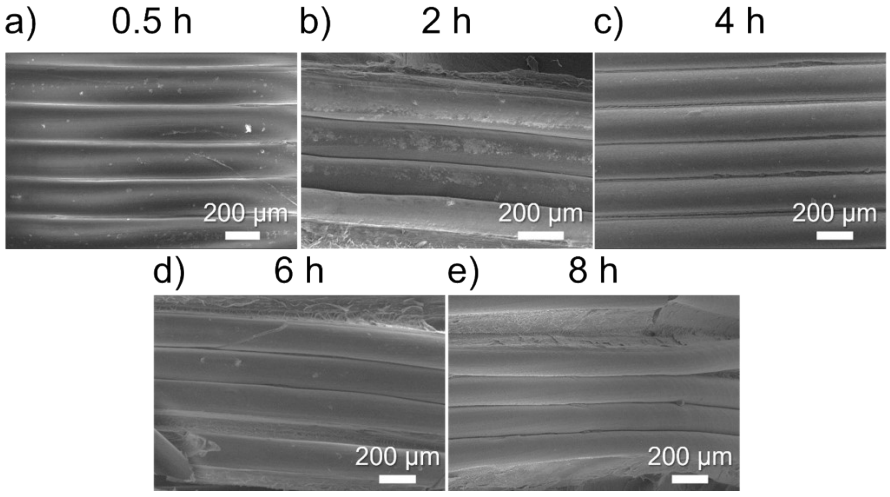

Figure S13. SEM micrograph of SEBS:PP (65:35 wt%) 3D-structures sulfonated at 135 °C for 0.5, 2, 4, 6, and 8 h.

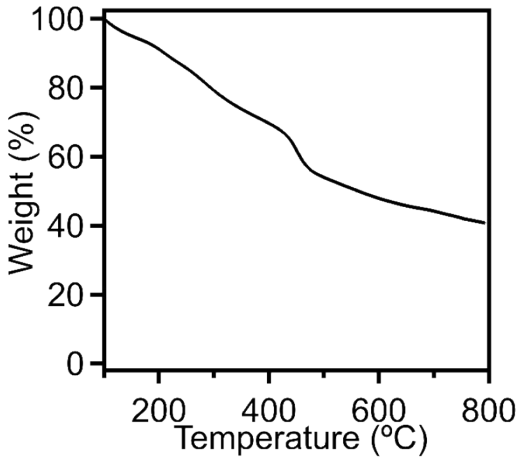

Figure S14. TGA thermogram up to 800 °C under nitrogen of sulfonated SEBS:PP (65:35 wt%) 3D-structure that was crosslinked for 8 h at 135 °C.

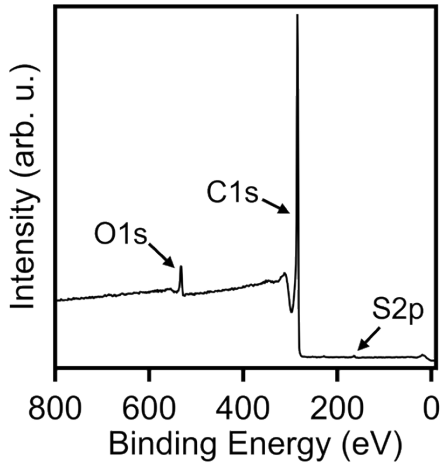

Figure S15. XPS survey scan of 3D-structured OMC.

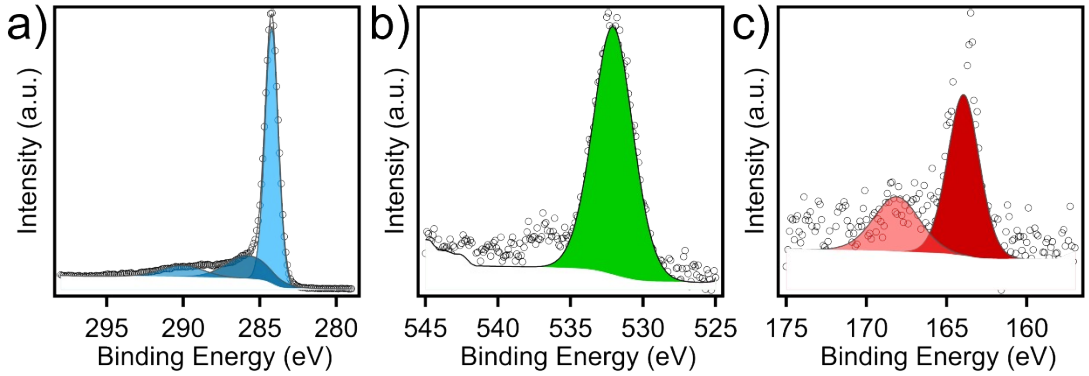

Figure S16. High-resolution XPS scans depicting (a) carbon (C1s), (b) oxygen (O1s), and (c) sulfur (S2p) bonding environments for the 3D OMC.

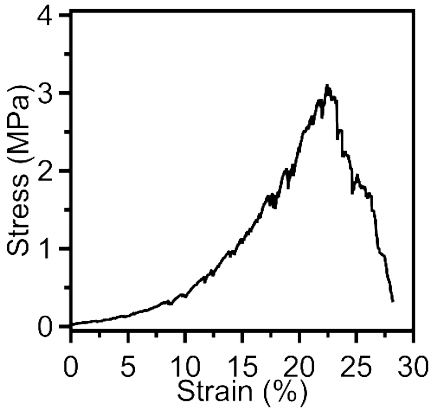

Figure S17. Representative compressive stress-strain curve of a 3D OMC prepared from a 65:35 wt% SEBS:PP blend.

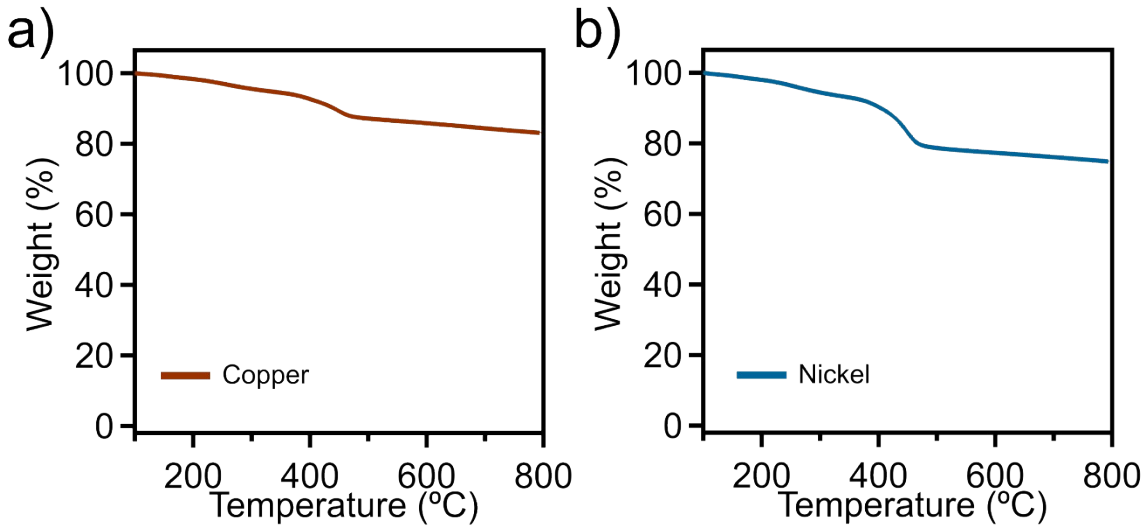

Figure S18. TGA thermogram up to 800 °C under nitrogen of the a) OMC-Cu nanocomposite and b) OMC-Ni nanocomposite.

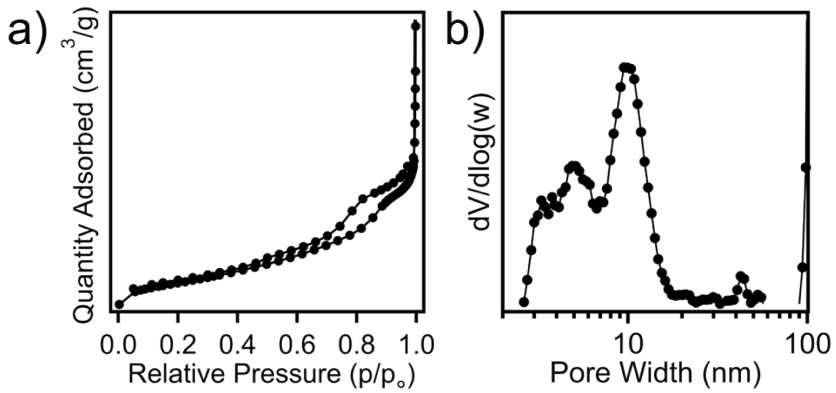

Figure S19. a) Nitrogen physisorption isotherm and b) pore size distribution of OMC-Cu nanocomposite.

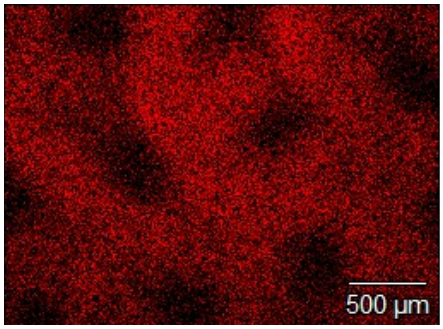

Figure S20. EDS copper elemental map for a cross-section of a 3D-structured OMC-Cu nanocomposite (copper in red).

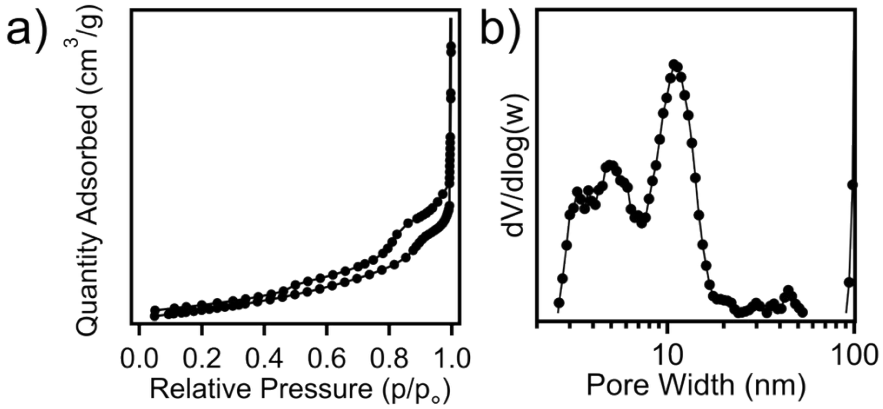

Figure S21. a) Nitrogen physisorption isotherm and b) pore size distribution of OMC-Ni nanocomposite.

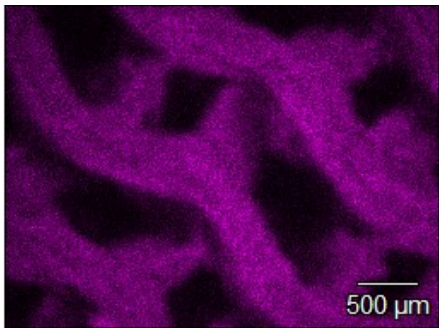

Figure S22. EDS nickel elemental map for a cross-section of a 3D-structured OMC-Ni nanocomposite (nickel in purple).

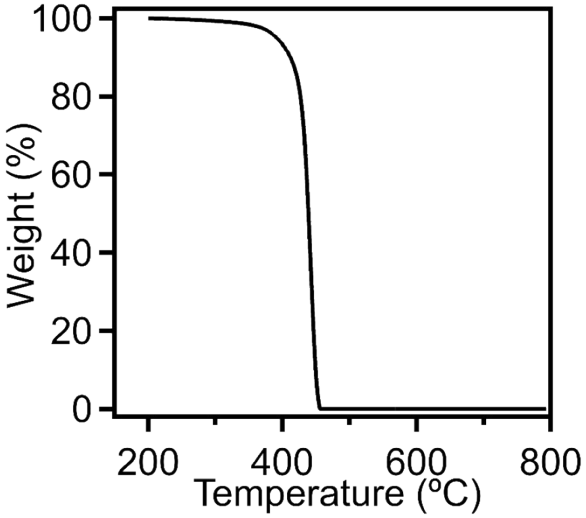

Figure S23. TGA thermogram up to 800 °C under air of the OMC.

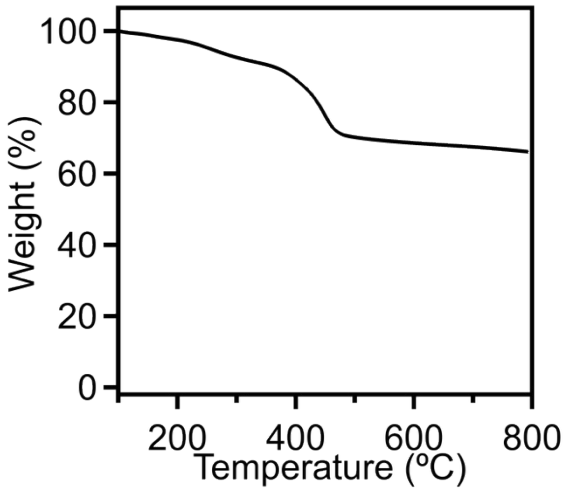

Figure S24. TGA thermogram up to 800 °C under nitrogen of the OMC-silica nanocomposite.

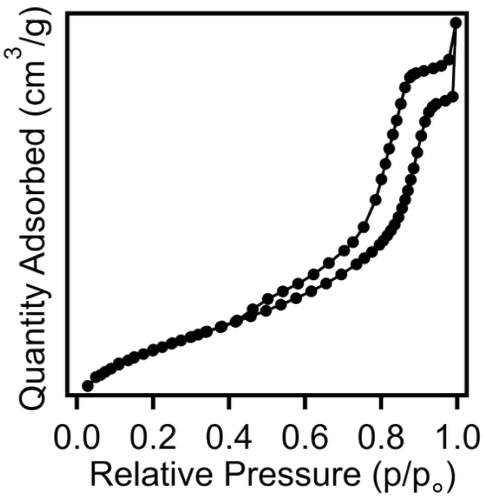

Figure S25. Nitrogen physisorption isotherm of OMC-Si nanocomposite (which was immersed in TEOS at 50 °C).

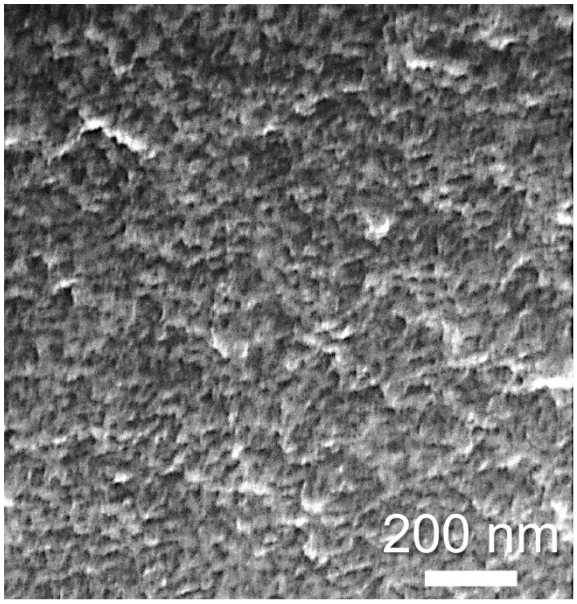

Figure S26. SEM micrograph of OMC-silica nanocomposite (which was immersed in TEOS at 50 °C).

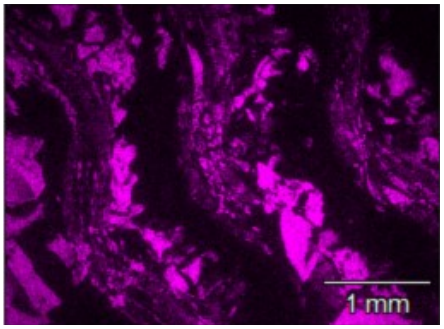

Figure S27. EDS silica elemental map for a cross-section of a 3D-structured OMC-silica nanocomposite (silica in purple).

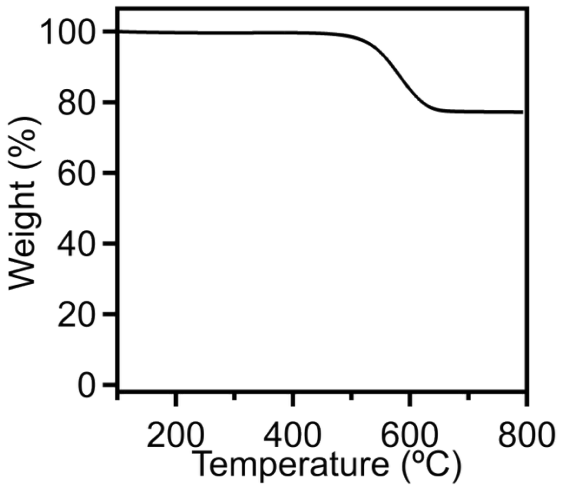

Figure S28. TGA thermogram up to 800 °C under air of highly-loaded OMC-silica nanocomposite (which was immersed in TEOS at 75 °C).

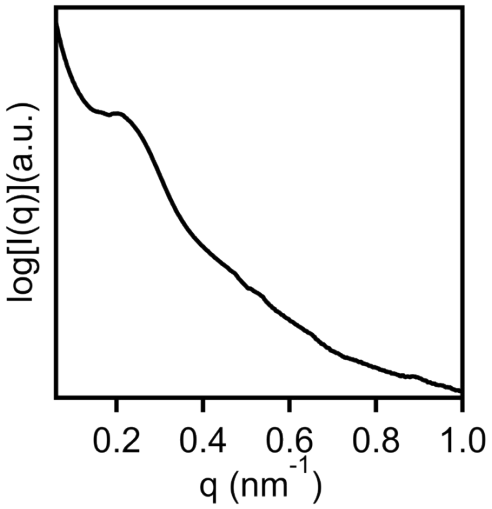

Figure S29. SAXS profile of highly-loaded OMC-silica nanocomposite (which was immersed in TEOS at 75 °C).

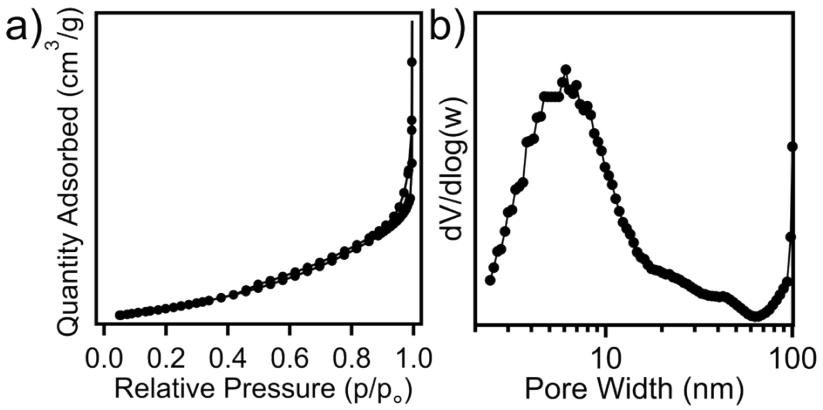

Figure S30. a) Nitrogen physisorption isotherm and b) pore size distribution of highly-loaded OMC-silica nanocomposite (which was immersed in TEOS at 75 °C).

Table S1. Comparison of pore textures for OMP as a function of reaction time.

Reaction time	Pore size (nm)	Micropore volume (cm^3/g)	Mesopore volume (cm^3/g)	Total pore volume (cm^3/g)
1 h	6.1	0.010	0.054	0.066
2 h	7.6	0.011	0.095	0.107
3 h	13.5	0.015	0.161	0.179
4 h	6.2	0.024	0.359	0.385

Table S2. Comparison of pore textures across different ordered mesoporous material matrix chemistries.

Sample	Surface area (m^2/g)	Pore size (nm)	Micropore volume (cm^3/g)	Mesopore volume (cm^3/g)	Total pore volume (cm^3/g)
OMP	-	13.5	0.010	0.161	0.179
OMC	379	11.5	0.068	0.332	0.400
OMC-Cu	364	11.3	0.078	0.472	0.550
OMC-Ni	374	9.9	0.050	0.259	0.309
OMC-Si	488	11.3	0.083	0.397	0.480